Spark ignition engine fuel-to-air ratio control: An adaptive control approach

Yildiray Yildiz [a,*], Anuradha M. Annaswamy [a], Diana Yanakiev [b], Ilya Kolmanovsky [b]

[a] Department of Mechanical Engineering, Massachusetts Institute of Technology, Cambridge, MA 02139, USA
[b] Department of Aerospace Engineering, The University of Michigan, Ann Arbor, MI 48109, USA

ARTICLE INFO

ABSTRACT

This paper presents the control of spark ignition (SI) internal combustion (IC) engine fuel-to-air ratio (FAR) using an adaptive control method of time-delay systems. The objective is to maintain the in-cylinder FAR at a prescribed set point, determined primarily by the state of the three-way catalyst (TWC), so that the pollutants in the exhaust are removed with the highest efficiency. The FAR controller must also reject disturbances due to canister vapor purge and inaccuracies in air charge estimation and wall-wetting (WW) compensation. Two adaptive controller designs are considered. The first design is based on feedforward adaptation while the second design is based on both feedback and feedforward adaptation incorporating the recently developed adaptive posicast controller (APC). Both simulation and experimental results are presented demonstrating the performance improvement by employing the APC. Modifications and improvements to the APC structure, which were developed during the course of experimentation to solve specific implementation problems, are also presented.

© 2010 Published by Elsevier Ltd.

1. Introduction

The fuel-to-air ratio (FAR) control performance can strongly impact key vehicle attributes such as emissions, fuel economy and drivability. For instance, the FAR in engine cylinders must be controlled in such a way that the resulting exhaust gases can be efficiently converted by the three-way catalyst (TWC). The TWC efficiency is about 98% when the fuel is matched to air charge in stoichiometric proportion and drops abruptly outside a narrow region. The TWC can also compensate for the temporary FAR deviation from stoichiometry, by either storing excess oxygen or releasing oxygen to convert excess hydro-carbons (HC) and carbon monoxide (CO). Thus, for the TWC to operate efficiently, the stored oxygen level must be regulated so that a range to accommodate further release or storage during transient conditions is available (Guzzella & Onder, 2004). In addition, the oxygen storage capacity of the TWC depends on the size and precious metal loading of the TWC. Therefore, if the FAR excursions and their durations are reduced with a well-performing controller, the storage capacity of TWC and its cost may be reduced as well.

The FAR control problem has been extensively investigated over many years. See for instance (Onder & Geering, 1993; Powell, Fekete, & Chang, 1998; Rupp, Onder, & Guzzella, 2008; Zhang, Grigoriadis, Franchek, & Makki, 2007) and references therein.

Main challenges in the design of the FAR controller include variable time delay, which is a key factor limiting the bandwidth of the feedback loop, uncertain plant behavior and disturbances. The plant uncertainties are the result of inaccuracies in the air charge estimation and in the wall-wetting (WW) compensation, as well as changes in the UEGO sensor due to aging. When the carbon canister, which stores the fuel vapor generated in the fuel tank, is purged, the fuel content in the purge flow into the intake manifold is also uncertain and creates disturbance to the FAR control loop.

Therefore, a control approach which can handle both uncertainties and large time-delays, and that can achieve a high performance is of interest. This work builds upon earlier literature by eliminating the need of a precise engine model for classical or optimization based algorithms and by eliminating the conservatism introduced by the robust control approaches. This is achieved by using the adaptive posicast controller (APC) (Yildiz, Annaswamy, Kolmanovsky, & Yanakiev, 2010), which is an adaptive controller for time delay systems. Successful adaptive control approaches are presented also in Ault, Jones, Powell, and Franklin (1994), Turin and Geering (1995), Jones, Ault, Franklin, and Powell (1995), Rupp et al. (2008), and Rupp (2009), but the approach presented in this paper is different from them: APC is based on direct adaptation where an online parameter identification scheme is not used and uncertainties are not confined to oxygen sensor parameters only but are allowed to appear elsewhere in the overall plant dynamics. In addition, APC is applied to a Lincoln Navigator test vehicle with eight cylinders, provided by Ford Motor Company, Dearborn, USA, which makes the control task much harder due to cylinder to cylinder

* Corresponding author. Tel.: +1 650 604 4382; fax: +1 650 604 4036.
E-mail addresses: yildiray.yildiz@nasa.gov (Y. Yildiz), aanna@mit.edu (A.M. Annaswamy), dyanakie@ford.com (D. Yanakiev), ilya@umich.edu (I. Kolmanovsky).

Nomenclature

F_c	fuel entering the cylinders
F_i	injected fuel
X	fraction of fuel contributing to the fuel puddle
τ_v	puddle evaporation time constant
Φ_{bm}	equivalence ratio right before measurement
Φ_{eng}	equivalence ratio right after the engine exit
τ_{gm}	gas mixing time constant
τ_{tr}	transport delay
τ	total delay
Φ_m	measured equivalence ratio
τ_s	sensor time constant
τ_m	reduced order model time constant
u_c	total control signal without WW compensation
u	feedback control input
F_b	base fuel
$(\frac{F}{A})$	desired fuel-to-air ratio
$\hat{A}$	estimated air mass flow rate
γ	adaptation gain
W_p	delay-free part of the plant transfer function
R_p	denominator polynomial of the plant transfer function
Z_p	numerator polynomial of the plant transfer function
k_p	high frequency gain of the plant transfer function
R_m	denominator polynomial of the reference model transfer function
k_m	high frequency gain of the reference model transfer function
A_p	plant state matrix
A_m	reference model state matrix
b_p	plant input vector
b_m	reference model input matrix
h_p	plant output vector
h_m	reference model output vector
Λ	signal generator state matrix
l	signal generator input vector
$(\cdot)^*$	ideal controller parameter
$(\tilde{\cdot})$	deviation from the ideal controller parameter
e	state error
e_1	output error
ω_1,ω_2	signal generator states
Ω	vector consisting of signal generator states and reference signal
α_1,α_2,k	finite dimensional controller parameters
λ	infinite dimensional controller parameter
θ	vector/scalar of finite dimensional controller parameters/parameter
Φ	equivalence ratio
Γ	adaptive gain matrix for finite dimensional parameters
γ_λ	adaptive gain for infinite dimensional parameters

variations. Finally, in this work, not only the APC results are presented but also a comparison with the existing control design in the test vehicle and with a gain scheduled Smith predictor (GSSP) are provided. It is noted that the GSSP used for comparison consists of a PI controller in series with a Smith block which predicts one delay interval ahead future output (FAR) of the engine. This future prediction is used as the feedback signal, which eliminates the effect of the time-delay to stability. In addition, the PI gains are scheduled according to the operating point of the engine. This combination of prediction and gain scheduling makes GSSP perform like a perfect "adaptive" controller. Therefore, the comparison of the APC with the GSSP presents how closely the APC is performing versus a high-performance controller.

The APC can be described as an adaptive controller that combines explicit delay compensation, using the classical Smith predictor (Smith, 1959) and finite spectrum assignment (Manitius & Olbrot, 1979), and adaptation (Ichikawa, 1985; Ortega & Lozano, 1988). As explained above, the Smith Predictor is simply a predictor that calculates one-delay-interval ahead future output of the plant by using the plant dynamics, to be used as the feedback signal. The Smith Predictor, however, has some disadvantages, one of which is unstable pole zero cancellations. Finite spectrum assignment controller solves this problem by using finite integrals in the future prediction. More details of the APC, Smith Predictor and finite spectrum assignment controller can be found in Yildiz et al. (2010). Due to such a unique combination, the APC effectively deals with both uncertainties and large time-delays both of which are dominant features of the FAR control problem. Previously, the authors explained preliminary implementation results of this controller to idle speed control and FAR control problems in conference papers (Yildiz, Annaswamy, Yanakiev, & Kolmanovsky, 2007; Yildiz, Annaswamy, Yanakiev, & Kolmanovsky, 2008a; Yildiz, Annaswamy, Yanakiev, & Kolmanovsky, 2008b). This paper expands on those results with further theoretical improvements, new experimental results and more detailed explanations of the experimental issues.

To fit the specific needs of the FAR application, APC design has been extended with additional features: First, an adaptive feedforward term is added which is crucial for disturbance rejection. Second, procedures are developed for the controller parameter initialization and the adaptation rate selection to reduce the calibration time and effort. Third, an algorithm to take care of the variable delay is introduced. Fourth, an anti-windup logic is used to prevent the winding up of the integrators used for parameter adaptation. Finally, a robustifying scheme is used to prevent the drift of the adaptive parameters. The main contribution of this work is the demonstration of the potential of this adaptive controller to improve the performance and to reduce the time and effort required for the controller calibration.

For comparison with the APC, in this paper a feedforward adaptive controller is also developed that attempts to minimize the impact of the purge fuel disturbance. This controller is also compared with the baseline controller using simulations and in-vehicle experiments.

While the control approach is adaptive, its development both benefits from and depends on the structural properties of the plant model. This model is briefly discussed next. The reader is referred to Guzzella and Onder (2004) for a more extended treatment of the underlying modeling techniques.

2. Plant model

The fuel–air ratio process dynamics are illustrated in Fig. 1 for which the reduced order model from the deviation in the commanded in-cylinder equivalence ratio to the measured equivalence ratio has the form (Yildiz et al., 2008b)

$$G(s) = \frac{1}{\tau_m s + 1} e^{-\tau s}. \tag{1}$$

3. Controller design

The structure of the closed loop system used in the test vehicle is presented in Fig. 2. The outer loop, consisting of the TWC, the HEGO sensor and the reference generator, determines the desired FAR, $(F/A)_d$, depending on the state of the TWC, measured by the HEGO sensor. All the other blocks that are not part of the outer loop form the inner loop. $(F/A)_d$ becomes the reference for the feedback controller, which is referred to as "Controller". The air estimate, referred to as $\hat{A}$, depends on the driver torque request. The multiplication of $(F/A)_d$ with $\hat{A}$ is referred to as the "base fuel", F_b, which is an estimate of the desired fuel. The feedback controller corrects this estimate using the UEGO sensor measurement of the FAR upstream of the TWC.

Feedback controller is the main focus of this paper. Two different adaptive controllers with different complexity are designed as feedback controllers. The baseline controller, which is the existing feedback controller in the vehicle, is explained first and then, adaptive controllers are presented.

3.1. Baseline controller

The baseline controller in the vehicle (see Fig. 2) is essentially a gain-scheduled proportional—plus—integral controller with output, u, modified to the total control signal (without WW compensation), u_c, according to following equation:

$$u_c = (1+u)F_b. \tag{2}$$

Note that, to maintain stability in the presence of delay, the gains of the PI controller cannot be made very aggressive. Moreover, due to the delay in the system, the overshoot in the response is difficult to avoid using this feedforward–feedback combination.

3.2. Adaptive feedforward controller (AFFC)

This is a simple model reference adaptive controller, where it is assumed that the only uncertainty occurs in the injector gain. Instead of the feedback path in Fig. 2, a gain multiplier on the $(F/A)_d$ is adapted (see Fig. 3). Note that the outer loop is not shown in the figure. The motivation for AFFC is to compensate for errors in the base fuel calculation due to, for example, injector uncertainties or "lost-fuel" effects present at cold engine conditions. Assuming that the desired FAR is in general constant and equal to stoichiometric FAR, it can be shown that this controller can also reject constant disturbances.

The adaptation law for the gain has the following form:

$$\dot{\theta} = \dot{\theta} = -\gamma er, \tag{3}$$

where γ is the adaptation rate and $e = (F/A)_m - (F/A)_{rm}$. Here $(F/A)_m$ and $(F/A)_{rm}$ represents the measured FAR and the output of the reference model.

Since AFFC avoids the asynchronous compensation from base fuel and feedback controller due to time delay and has only one parameter, it is easy to tune and it provides more damped response to reference changes compared to the baseline controller.

3.3. Adaptive posicast controller (APC)

APC (Yildiz et al., 2010) is a model reference adaptive controller for systems with unknown dynamics (not limited to just a gain as in AFFC case) and a known input delay, which are modeled by the following input–output description

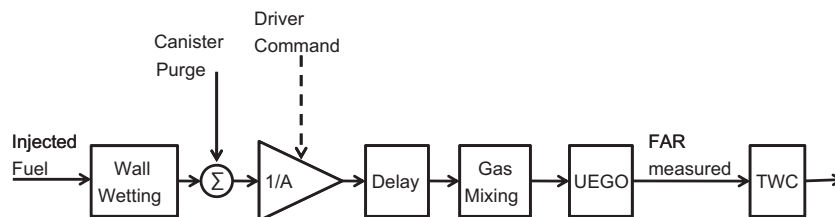$$y(t) = W_p(s)u(t-\tau), \quad W_p(s) = \frac{k_p Z_p(s)}{R_p(s)}, \tag{4}$$
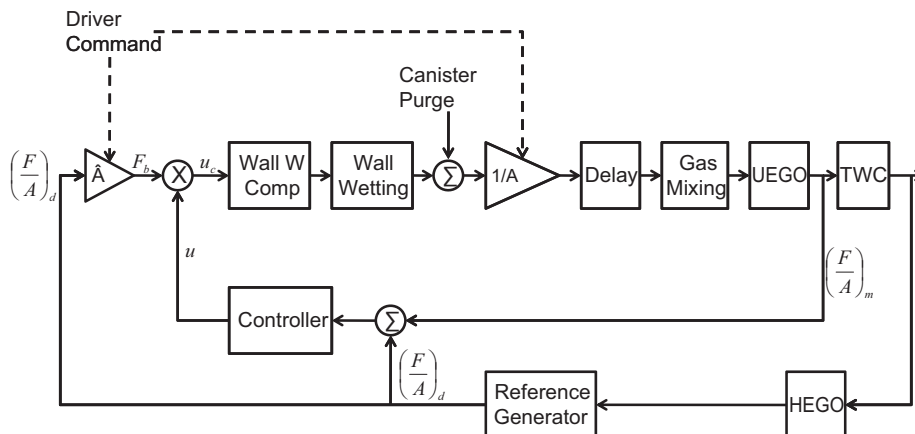

Fig. 1. Plant block diagram representation.

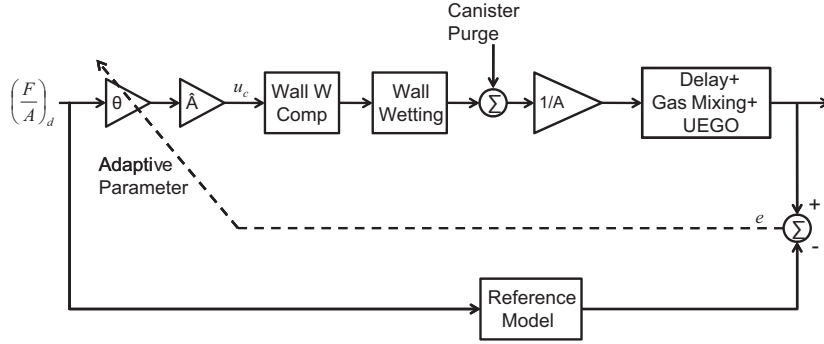**Fig. 2.** Overall closed loop controller structure.

Fig. 3. Inner-loop structure with AFFC.

where y is the measured plant output, u is the control input, and $W_p(s)$ is the delay-free part of the plant transfer function. $R_p(s)$ is the nth order denominator polynomial, not necessarily stable and the numerator polynomial, $Z_p(s)$ has only minimum phase zeros. The relative degree, n^*, which is equal to the order of the denominator minus the order of the numerator, is assumed to be smaller or equal to two. It is also assumed that the delay and the sign of the high frequency gain k_p are known, but otherwise $W_p(s)$ may be unknown. Suppose that the reference model, reflecting desired response characteristics, is given as

$$y_m(t) = W_m(s)r(t-\tau), \quad W_m(s) = \frac{k_m}{R_m(s)}, \tag{5}$$

where $R_m(s)$ is a stable polynomial with degree n^*, k_m is the high frequency gain and r is the desired reference input.

Consider the following state space representation of the plant dynamics (4), together with two "signal generators" formed by a controllable pair Λ, l

$$\dot{x}_p(t) = A_p x_p(t) + b_p u(t-\tau), \quad y(t) = h_p^T x_p(t), \tag{6}$$

$$\dot{\omega}_1(t) = \Lambda \omega_1(t) + l u(t-\tau), \tag{7}$$

$$\dot{\omega}_2(t) = \Lambda \omega_2(t) + l y(t), \tag{8}$$

where $\Lambda \in \Re^{n \times n}$ and $l \in \Re^n$. It is noted that signal generators act like state observers and typically seen in output feedback adaptive control schemes.

Now, the control of the plant (4) is considered when the transfer function $W_p(s)$ has unknown coefficients and the time delay τ is known. Consider the following adaptive controller (Yildiz et al., 2010):

$$u(t) = \alpha_1(t)^T \omega_1(t) + \alpha_2(t)^T \omega_2(t) + \int_{-\tau}^{0} \lambda(t,\sigma)u(t+\sigma)\,d\sigma + k(t)r(t),$$

$$\dot{\theta}(t) = -\Gamma e_1(t)\Omega(t-\tau),$$

$$\frac{\partial \lambda(t,\sigma)}{\partial t} = -\gamma_\lambda(\sigma)e_1(t)u(t+\sigma-\tau), \tag{9}$$

where

$$\theta = \begin{bmatrix} \alpha_1 \\ \alpha_2 \\ k \end{bmatrix}, \quad \Omega = \begin{bmatrix} \omega_1 \\ \omega_2 \\ r \end{bmatrix}, \quad e_1 = y - y_m, \tag{10}$$

Γ is a diagonal matrix, the entries of which represent the adaptation rate of the corresponding controller parameter and $\gamma_\lambda(\sigma)$ is the adaptation rate for the controller parameter $\lambda(t,\sigma)$.

It can be shown Yildiz et al. (2010) that the plant (4), adaptive controller and the adaptive laws given in (9) have bounded solutions for all $t \geq t_0$ and $\lim_{t \to \infty} e_1(t) \to 0$.

3.4. Implementation enhancements

Below, several issues, which were not taken into account during the initial design but arise in the implementation, and how they are addressed are explained.

3.4.1. Disturbance rejection
Controller (9) is designed without taking input disturbances into account, while disturbance rejection is one of the basic requirements of the FAR control problem. By modifying the arguments in Yildiz et al. (2010) it can be shown that the feed-forward term $k(t)r(t)$ behaves as an integrator and that the controller is able to reject constant input disturbances (Yildiz, 2009).

3.4.2. Initialization and adaptation rate selection
Controller parameters are initialized by satisfying the model matching using a nominal plant model (700 rpm at warm idling conditions). Idling is considered as the worst case since the delay value achieves its maximum. In this operating condition τ and τ_m is found to be 0.4 and 0.45, respectively.

Defining $\bar{\theta} = [\alpha_1 \; \alpha_2 \; \lambda_1 \; \ldots \; \lambda_m \; k]^T$, where $\lambda_1 \; \ldots \; \lambda_m$ correspond to the discretization of $\lambda(\cdot, \sigma)$ (see (12)) the adaptation gain $\bar{\Gamma}_{ii}$ for a particular controller parameter $\bar{\theta}_i$ is chosen using the following empirical rule:

$$\bar{\Gamma}_{ii} = c\bar{\theta}_{i0}, \tag{11}$$

where c is an adjustable gain and $\bar{\theta}_{i0}$ is the initial value of the corresponding controller parameter. The same c is used for all the parameters which makes the fine tuning procedure easy and fast. The rationale for this rule is to make all the controller parameters equally effective in the control law.

3.4.3. Approximation of the finite integral term
The finite integral term in the control signal u given in (9) is implemented by using a set of point-wise delays (Manitius & Olbrot, 1979) as in the following:

$$\int_{-\tau}^{0} \lambda(\sigma,t)u(t+\sigma)\,d\sigma = \lambda_1(t)u(t-dt) + \cdots + \lambda_m(t)u(t-m\,dt), \tag{12}$$

where dt is the sampling interval and $m\,dt = \tau$. See in Yildiz, Annaswamy, Yanakiev, and Kolmanovsky (accepted for publication, Appendix C) where it is shown that the danger of instability due to this approximation does not arise for the FAR implementation.

3.4.4. Handling time-varying delay
In the design of the APC, it assumed that the time delay in the system is known and constant. However, the time delay in the FAR control problem varies with the load and the speed of the engine. A logical way of handling this issue is gain-scheduling the controller,

time delay being the gain-scheduling variable. The delay value shows itself in the Eq. (7) and in the adaptation laws given in (9), which are straightforward to gain-schedule. Apart from these, the finite integral term in the control law given in (9) also needs the delay information to be computed. Note that an approximation is used for this term given in (12). Two different strategies are pursued to gain-schedule this approximation, which are given below:

(a) *Eliminating and adding terms*: The integral in (12) is approximated using time steps that are equal to the sampling interval, dt, of the controller implementation ($dt = 30$ ms). Therefore, the number of the terms, m, in this approximation can be given as $m = \tau/T$. A simple way to gain-schedule this approximation is to eliminate or add terms, depending on the value of the delay at the time of approximation. One can do this by storing the values of eliminated parameter λ_i's when the delay decreases and then using these stored values when the number of the terms increases again, due to a delay increase.

Although this logic seems intuitive, it has a drawback of rapid control signal changes that can cause undesired excursions in the FAR trace.

(b) *Freezing and reactivating terms*: To prevent the undesired excursions in the FAR trace, instead of eliminating the unnecessary terms, $\lambda_i(t)u(t - i\,dt)$'s, they are simply frozen and used back when the delay value increases. This strategy achieves two things: First, it still makes sure that only the necessary terms are being used and thus only the necessary parameter λ_i's are being updated, while the rest of them are frozen. Second, by still keeping the frozen terms in the control signal, it leads to a smooth transition from one delay approximation to another.

3.4.5. Anti-windup logic

An add-on algorithm needs to be integrated with the controller that prevents the winding up of the integrators resulting from the adaptation laws in (9).

Anti-windup logic is used where the main goal is to stop the adaptation if the control signal saturates and if the tracking error, $e_1 = y_m - y$, is not favorable, i.e., if the error does not have a sign that would force the integrators to unwind. Calling the control signal before the saturation block as u and after the saturation as u_{sat}, the anti-windup algorithm can be expressed as in the following:

$$\dot{\overline{\theta}}_i(t) = \begin{cases} 0 & \text{if } u > u_{sat} \quad \text{and} \quad e_1 < 0 \\ & \text{or} \\ & u < u_{sat} \text{ and } e_1 > 0, \\ -\overline{\Gamma}_{ii}e_1(t)\overline{\Omega}_i(t-\tau) & \text{otherwise}. \end{cases} \tag{13}$$

3.4.6. Robustness

Due to possible violations of the assumptions in the controller design, the controller parameters may drift without converging to a bounded region. One of the remedies to this problem is using $\sigma-$modification robustness scheme (Narendra & Annaswamy, 2005), which mainly adds a damping term to adaptation laws as in the following:

$$\dot{\overline{\theta}}(t) = -\overline{\Gamma}e_1(t)\overline{\Omega}(t-\tau) - \sigma\overline{\theta}(t), \tag{14}$$

where σ is a constant. The authors previously used this robustness scheme in idle speed control application (Yildiz et al., accepted for publication)) which proved successful and therefore it is used again in FAR control application. See Yildiz et al. (accepted for publication) for the details.

4. Simulation and experimental results

The simulation results in this section are obtained using ®Matlab and ®Simulink, and the experimental results are obtained using a Lincoln Navigator test vehicle provided by Ford Motor Company. The vehicle has a 5.4l V-8 front engine with a multi-port fuel injection system. The engine has three valves per cylinder and can achieve 300 Hp at 5000 rpm and 495 N m at 3750 rpm. The air intake is controlled with an electronic throttle.

A dSPACE MicroAutoBox, communicating with the engine control unit (ECU) via CAN bus was used for real-time controller rapid prototyping. Fig. 4 shows the hardware wiring.

In the experimental setup, the FAR control commands coming from the ECU are overridden with the adaptive control signal by using the rapid prototyping system (see Fig. 4). This system receives the FAR measurement and calculates the fuel mass flow rate as the control input.

The existing closed loop control structure in the vehicle is presented in Fig. 2. The adaptive controller overwrites the "Controller" block, while the rest of the structure is retained as is. Thus, the presented results compare the performance of the existing feedback controller in the test vehicle with the adaptive controller. It was observed that the adaptive posicast controller performed better, in terms of a predefined success measure, when compared to the existing baseline controller, in all experiments.

4.1. AFFC vs. baseline controller

Fig. 5 compares the tracking and purge disturbance rejection performance of the baseline controller and of the AFFC when WW
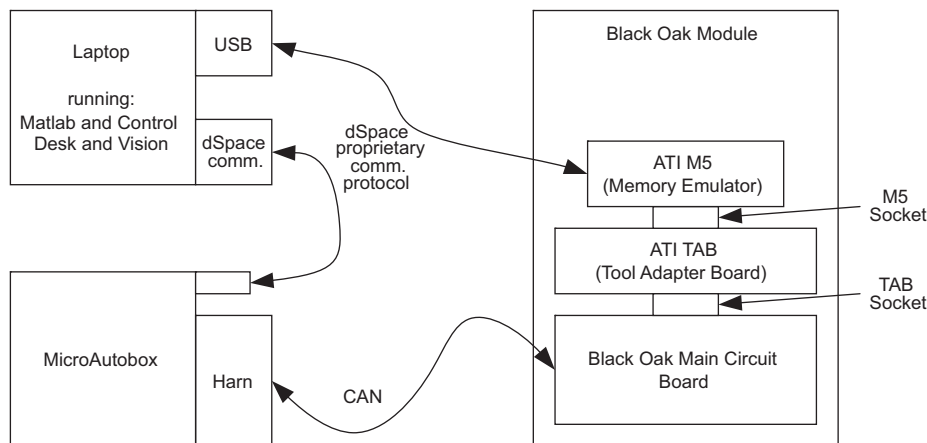

Fig. 4. Rapid prototyping with MicroAutobox using CAN.

dynamics are assumed to be perfectly compensated. Φ denotes the normalized FAR or the equivalence ratio (so that stoichiometric FAR of 0.0685 corresponds to $\Phi = 1$). The upper plot shows the simulated response to a pulse train reference and the lower plot shows the response to a step purge disturbance introduced at time $t = 30$ s and removed at time $t = 50$ s. It is assumed that the time delay is known to be 0.4 s. While designing the AFFC, the UEGO dynamics are assumed to have nominal values but then the plant dynamics were chosen to have 20% deviations in high frequency gain and τ_m. The baseline controller is tuned to perform well for both tracking and disturbance rejection. As discussed before, the baseline controller cannot avoid overshoots due to the delay in the system, while the AFFC can track the reference comparatively better. On the other hand, the disturbance rejection capabilities are similar, since when the reference is constant, the AFFC is essentially an integral controller. It is noted that the plots presented shows the response after $t = 30$ s when the adaptive gain has already reached to a certain bounded interval.

AFFC is also tested experimentally and compared with the existing baseline controller. At the test time, the calibration of WW compensation was not fully completed, which allowed to subject both controllers to challenging scenarios. Also, the time delay varied in the experiments as opposed to the cases simulated in Fig. 5. Fig. 6 shows the results from a 4-min drive test. Note that the air charge values have been scaled to show them in the same plot with Φ. The test was conducted in a relatively uncontrolled environment, e.g., without controlling the speed or load, as can be observed in Figs. 6a–c. The vehicle was accelerated and decelerated rather sharply and the purge flow was also not controlled, as shown in Fig. 6d. Fig. 6e shows a 5-s window zoomed from Fig. 6b. The RMS error value of the deviations from the reference is calculated as 0.0052 and 0.0051 for the baseline controller and for the AFFC, respectively. Their performances are
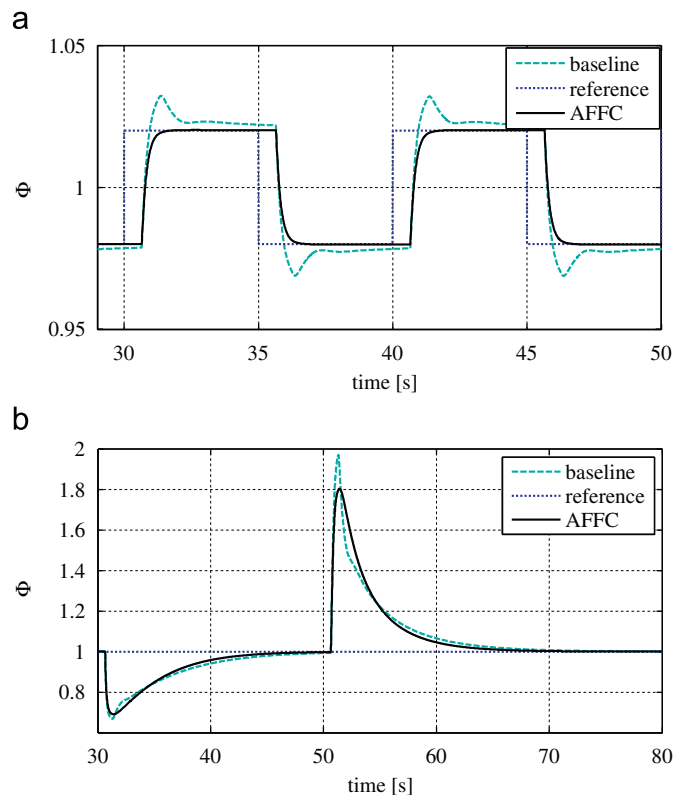
similar, consistent with the simulation results, as the dominant factors affecting the response are the purge and air disturbances, and not the reference tracking.

Note that another important success measure (SM) for the FAR control loop is the error integral. Compared to RMS error, this metric better reflects how much of the TWC oxygen storage capacity is used to compensate for the deviations in the fuel-to-air ratio.

The integral error SM can be formulated as

$$SM = \frac{1}{k} \sum_{i=1}^{k} \left| \int_{t_i}^{t_i + \Delta_i} e_1(\eta) \, d\eta \right|, \tag{15}$$

where t_i is the time instant of the i-th disturbance hit, Δ_i is the duration/settling time of the transient caused by the disturbance hit and k is the number of times that the disturbance is introduced. This SM is used for the APC results in the following sections.

4.2. APC vs. baseline controller

4.2.1. Purge disturbance rejection tests

The purpose of initial FAR control experiments was to compare the performances of the APC and the baseline controller, while emulating canister vapor purge disturbance rejection tests. These experiments were conducted with the test vehicle idling at different speeds. These different idling speeds were obtained by changing the idle speed set point in the ECU code. Since during idling the air flow rate does not change much, the WW dynamics did not play a major role in these experiments as much as it did for acceleration and deceleration experiments. The SM used is given in (15).

The test started with the engine speed at 700 rpm. At 300 s, the engine speed increased to 1000 rpm and at 600 s it decreased back to 700 rpm. Every 20 s the fuel injector gains were changed to emulate the purge disturbance. Overall, the performance of the APC, calculated using (15), was 70% better than the baseline controller during the test which lasted 15 min. Fig. 7 shows a time window from the test where the engine speed was 700 rpm. The APC performs considerably better, in terms of integral SM, than the baseline controller as its features enable it to better account for the delay and achieve faster response.

Fig. 8 shows how the equivalence ratio changes during the same test but now the engine speed is 1000 rpm. Again, the performance of the APC is better than that of the baseline controller. It is noted that during all these tests the idle speed was controlled by a separate controller in the engine control unit, via the air mass flow rate. Also, the experiments were conducted at warm conditions in quick successions. Therefore, the factors affecting the system dynamics, engine speed, load and coolant temperature did not show any meaningful differences for different controller runs. This shows that the performance differences were mainly due to controllers.

4.2.2. Acceleration and deceleration tests

Fig. 9 shows the equivalence ratio excursions during a test in which the vehicle accelerates and then decelerates. In this case, the delay varies with time during the test. The APC performs better overall than the baseline controller. During the lean excursion (equivalence ratio less than 1 during acceleration), the baseline controller appears to start the recovery from the undershoot slightly earlier than the APC. There is, however, a difference in the equivalence ratio set-point time of increase between APC test and baseline controller test, further analysis of these suggests no real advantage for the baseline controller over APC in terms of start of recovery timing. Note that the equivalence ratio set-point is computed by a separate part of the engine
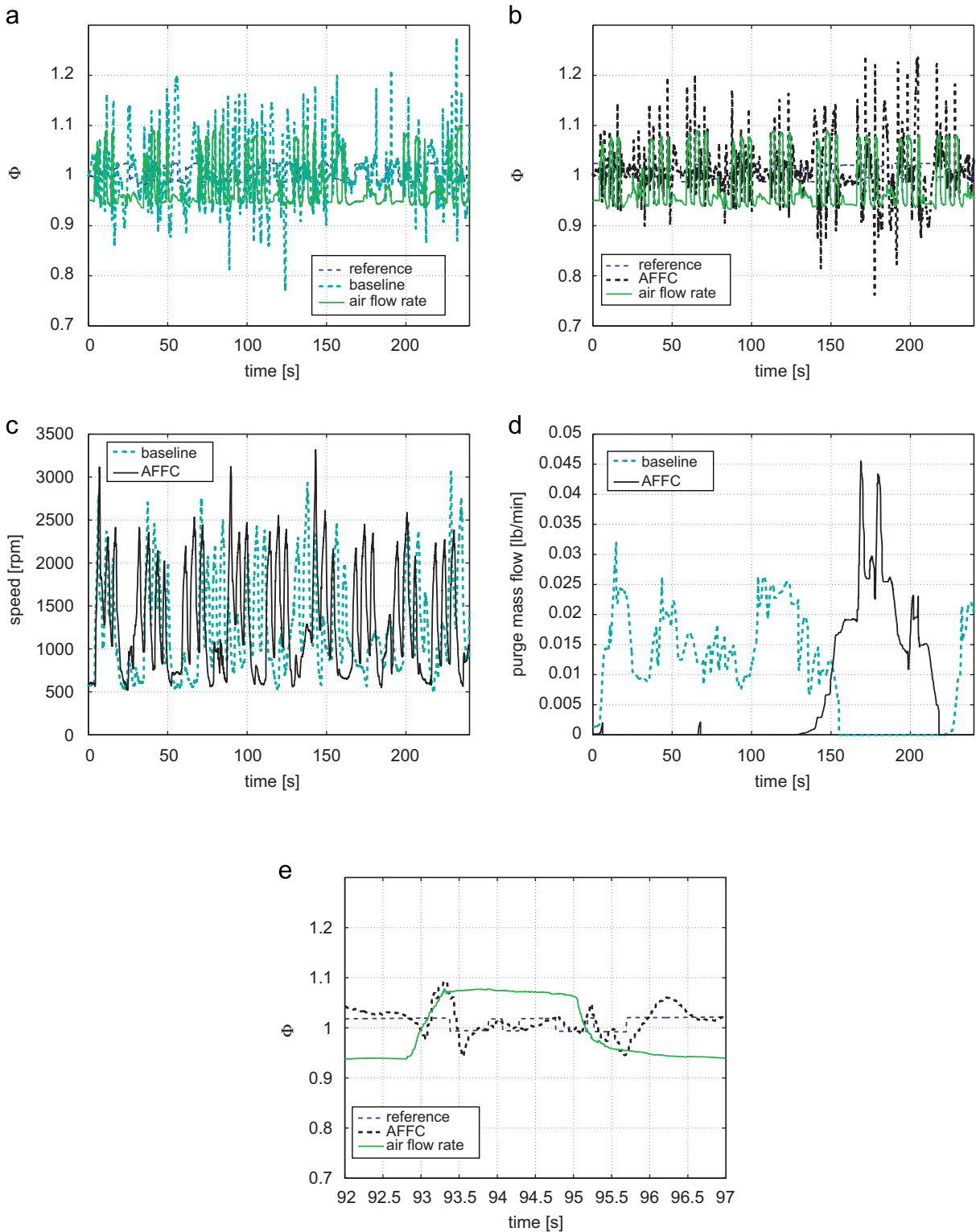

Fig. 5. Comparison of baseline controller and AFFC: (a) response to a set-point change and (b) response to purge disturbance (simulation).

Fig. 6. Baseline controller vs. AFFC: (a) Φ and air flow rate when baseline controller is active; (b) Φ and air flow rate when AFFC is active; (c) engine speeds; (d) purge fuel flow rates; and (e) 5-s window zoomed from subfigure (b) (experiment).

control system in the vehicle. It is also noted that the engine speed and load were almost identical with the exception of a small difference of the air flow during the first second of the experiment. The experiments were conducted in quick successions at warm conditions so engine coolant temperatures (ECTs) were also almost the same. Therefore, the performance differences were due to controllers.

For this experiment, the maximum value of the integrated difference between fuel–air equivalence ratio and its set point are compared during the full course of the experiment. This metric is better suited to assessing the difference between controllers for this experiment than (15) because if one acceleration-deceleration test is assumed to be a single event, the errors cancel each other if (15) is used, which can be observed in Fig. 9d. However,
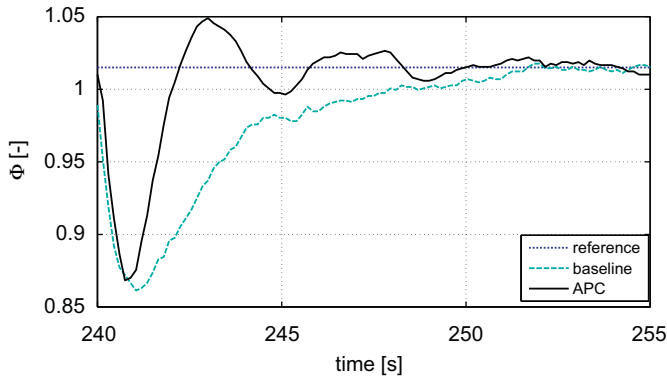
Fig. 7. Comparison of baseline controller with APC for purge disturbance rejection at 700 rpm (experiment).
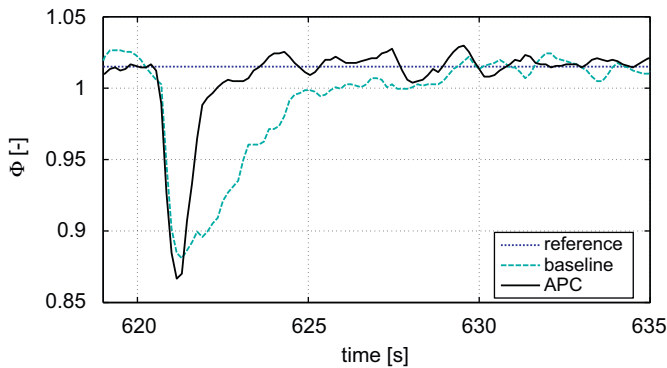

Fig. 8. Comparison of baseline controller with APC for purge disturbance rejection at 1000 rpm, with $c=1$ (experiment).

maximum value of the integral relates to how much of the oxygen storage capacity is used in the worst case during the course of the experiment. In terms of this metric, APC performs 43% better than the baseline controller.

All the above experiments were conducted with the fine tuning parameter c equal to 1, which implies that no fine-tuning was done. In Fig. 10, an experimental result, which shows APC and the baseline controller performances during the vehicle acceleration, is presented with $c=1.5$. As expected, the APC outperforms the baseline controller to a greater extent compared to the previous cases, especially on lean excursions. Note, however, that the load (and hence the air charge) are less in the APC controller case in this experiment. Nevertheless, performance with the APC is considerably better than with the baseline controller, and cannot be attributed to the load difference between the controllers.

4.3. APC vs. gain-scheduled smith predictor

The performance of the APC was compared with a gain-scheduled Smith Predictor (SP). The SP was designed based on the plant models identified at different operating points (corresponding to different combinations of engine speeds and loads) using a relay feedback method.

Fig. 11 shows the results of an acceleration-deceleration test conducted using the test vehicle. The performances are very similar as can be seen in Fig. 11a and d, where the time evolutions of Φ and the error integral is presented. On the other hand, Fig. 11c shows that the control signal of the APC is smoother than that of the SP. Time history of α_{21}, which is the first component of the controller parameter vector α_2, is presented in Fig. 11e.
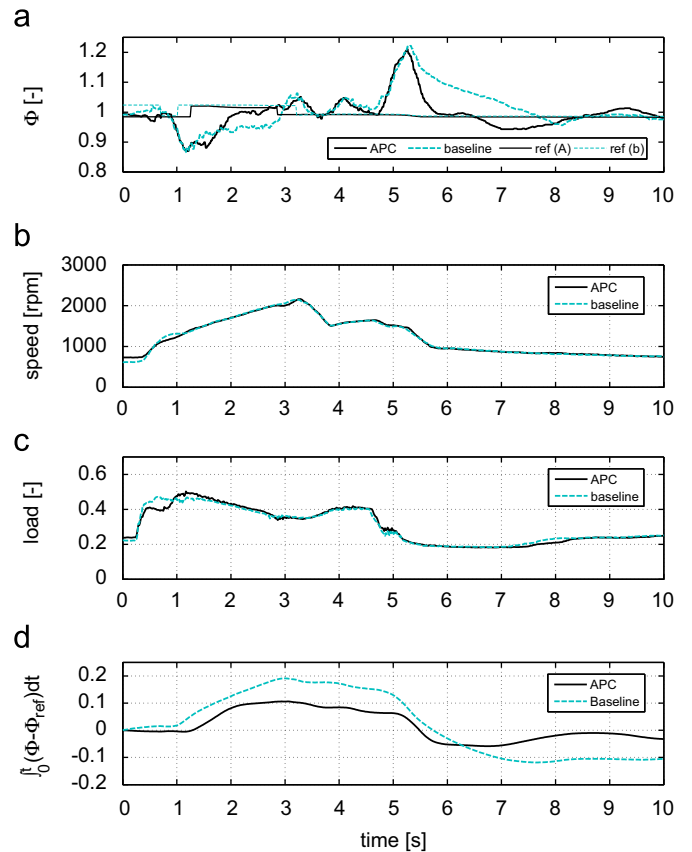

Fig. 9. Time histories of: (a) Φ, (b) engine speed, (c) engine relative air flow, (d) tracking error integral, during vehicle acceleration and deceleration for APC vs. baseline controller, with $c=1$ (experiment).
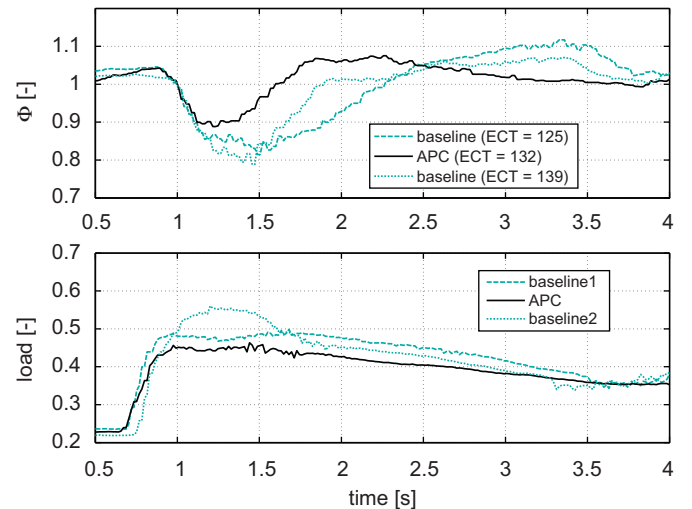

Fig. 10. Comparison of baseline controller with APC during vehicle acceleration, with $c=1.5$. ECT stands for engine coolant temperature (experiment).

Fig. 11 confirms that the adaptive controller is similar in performance to the Smith Predictor. Note that the gain-scheduled SP can be seen as a perfect adaptive controller: While the APC adapts to operating point changes without the knowledge of the plant parameters, the gain-scheduled SP uses the knowledge of the changing plant parameters that need to be obtained offline by using an identification procedure for different operating points. The adaptive controller can, in addition, adjust better to situations
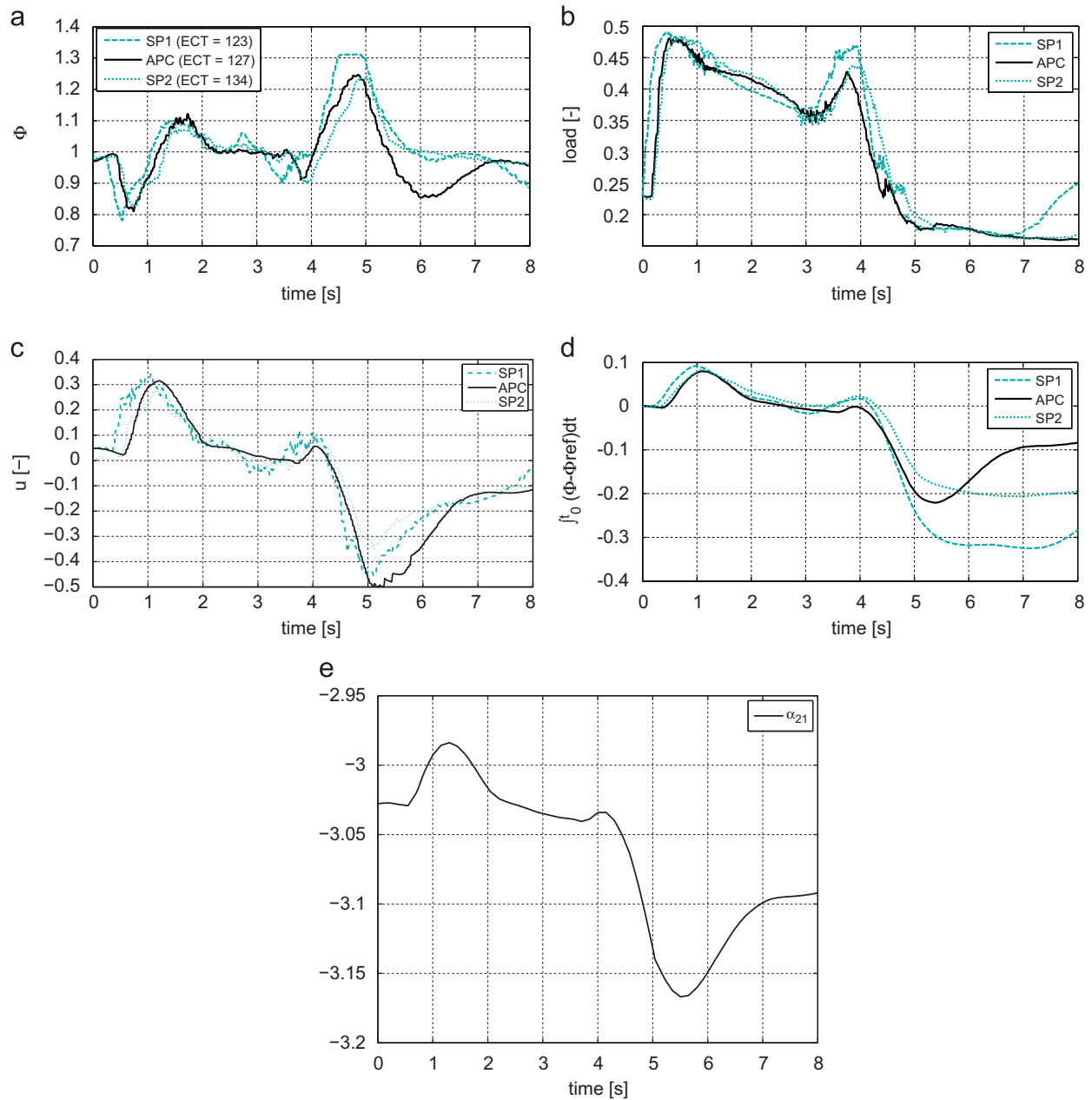
Fig. 11. Time histories of: (a) Φ (ECT stands for engine coolant temperature), (b) engine relative air flow, (c) feedback control input, (d) tracking error integral, during vehicle acceleration and deceleration for gain-scheduled SP vs. APC, with $c = 1.5$, and (e) evolution of the first component of α_2 (experiment).

when plant parameters change due to part-to-part variability or aging. For example, it is stated in Rupp et al. (2008) that due to aging or harsh operating conditions, UEGO sensor time constant can increase by a factor of 10–20. Also it is known that the Smith predictor is sensitive to the delay estimation errors (Niculescu, 2001).

In Fig. 12, simulation results that compare SP with APC are presented. For this simulation, the time constant for the first order system model is selected as 50 ms, which is reported in Rupp et al. (2008) as the time constant of a state-of-the-art oxygen sensor. The nominal time delay is assumed to be 0.4 s. A step input disturbance is introduced to this plant at time $t = 170$ s and the transients are plotted. The APC and the SP is tuned such that they perform similarly for these nominal plant parameter values, in the presence of the disturbance. Then, the sensor time constant is increased by a factor of 20 and the disturbance test is repeated.
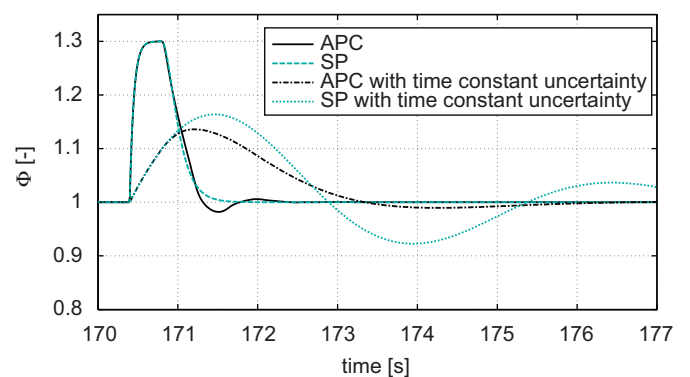

Fig. 12. Comparison of SP and APC for input step disturbance rejection in the presence of sensor time constant uncertainty (simulation).
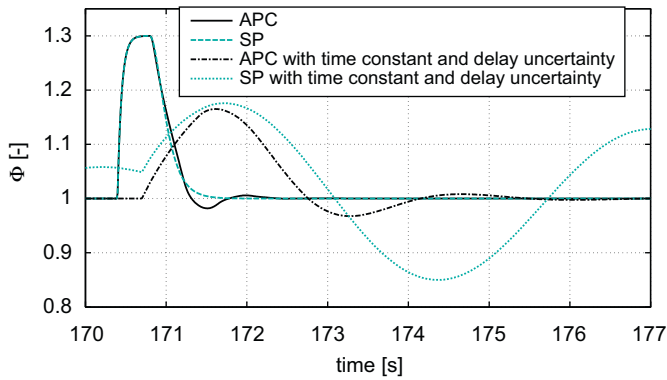
Fig. 13. Comparison of SP and APC for input step disturbance rejection in the presence of sensor time constant and delay uncertainty (simulation).

As seen in the figure, not only the performance of the SP gets worse than the adaptive controller, but the SP response also becomes oscillatory, which is a sign of getting closer to instability. An additional uncertainty in the system, like a delay identification error, may cause the system to become unstable easily. Indeed, when a delay uncertainty is introduced by increasing the nominal delay by 0.3 s, it is seen that the loop with the SP starts to show a lightly damped response (with a damping ratio of approximately 0.03) with large oscillations which shows that the closed loop poles get close to the imaginary axis. This simulation result is presented in Fig. 13.

5. Summary

In this paper, the fuel-to-air ratio (FAR) control problem in port-fuel-injection (PFI) spark-ignition (SI) engine is considered. Two controllers, an Adaptive FeedForward Controller (AFFC) and an Adaptive Posicast Controller (APC), have been developed and implemented in a test vehicle. The AFFC is a simple controller based on feedforward adaptation, while the APC is a more elaborate controller that uses adaptation in both feedforward and feedback paths and is based on a recently developed adaptive control method for time-delay systems. The AFFC has been shown in simulations and experiments to have better reference tracking and similar disturbance rejection capabilities when compared to the existing baseline controller. The APC has been shown in experiments to achieve faster recovery from disturbances and better performance during vehicle acceleration deceleration tests. These performance improvements were a result of various modifications and enhancements to the initial APC design, such as an algorithm to handle the variable time delay, a robustness scheme and parameter initialization and fine tuning methods. It has also been observed in vehicle experiments that implementing APC using an upper bound on the delay as a delay estimate assures robustness against delay variations.

In terms of applications of the APC, the FAR control problem is more challenging than the Idle Speed Control (ISC) problem, which the authors of this paper have treated in Yildiz et al. (2007) and Yildiz et al. (accepted for publication), due to a larger and variable time delay and different character of disturbances and uncertainties. The experimental results reported here demonstrate that the APC is effective for the FAR control problem as well.

References

Ault, B., Jones, V. K., Powell, J. D., & Franklin, G. F. (1994). Adaptive air–fuel ratio control of a spark-ignition engine. *SAE paper* (940373).
Guzzella, L., & Onder, C. H. (2004). *Introduction to modeling and control of internal combustion engine systems* (1st ed.). Springer.
Ichikawa, K. (1985). Frequency-domain pole assignment and exact model-matching for delay systems. *International Journal of Control*, 41, 1015–1024.
Jones, V. K., Ault, B. A., Franklin, G. F., & Powell, J. D. (1995). Identification and air–fuel ratio control of a spark ignition engine. *IEEE Transactions on Control Systems Technology*, 3(1).
Manitius, A. Z., & Olbrot, A. W. (1979). Finite spectrum assignment problem for systems with delays. *IEEE Transactions on Automatic Control*, 24(4).
Narendra, K. S., & Annaswamy, A. M. (2005). *Stable adaptive systems*. New York: Dover Publications.
Niculescu, S. I. (2001). *Delay effects on stability: a robust control approach*. Heidelberg, Germany: Springer-Verlag.
Onder, C. H., & Geering, H. P. (1993). Model-based multivariable speed and air-to-fuel ratio control of an SI engine. *SAE paper* (930859).
Ortega, R., & Lozano, R. (1988). Globally stable adaptive controller for systems with delay. *International Journal of Control*, 47(1), 17–23.
Powell, J. D., Fekete, N. P., & Chang, C. F. (1998). Observer-based air–fuel ratio control. *IEEE Control Systems Magazine*, 18(5), 72–83.
Rupp, D. (2009). *Model-based adaptive air/fuel ratio control for an automotive gasoline engine*. Ph.D. thesis, ETH Zurich, February.
Rupp, D., Onder, C., & Guzzella, L., 2008. Iterative adaptive air/fuel ratio control. In *Proceedings of the advances in automotive control*, Seascape Resort, USA.
Smith, O. J. (1959). A controller to overcome dead time. *ISA Journal* 6.
Turin, R., & Geering, H. (1995). Model-reference adaptive A/F ratio control in an SI engine based on Kalman-filtering techniques. In *Proceedings of the American control conference* (pp. 4082–4090).
Yildiz, Y. (2009). *Adaptive control of time delay systems and applications to automotive control problems*. Ph.D. thesis, Massachusetts Institute of Technology.
Yildiz, Y., Annaswamy, A., Kolmanovsky, I., & Yanakiev, D. (2010). Adaptive posicast controller for time-delay systems with relative degree $n^* \leq 2$. *Automatica*, 46(2), 279–289.
Yildiz, Y., Annaswamy, A., Yanakiev, D., & Kolmanovsky, I. (2007). Adaptive idle speed control for internal combustion engines. In *Proceedings of the American control conference* (pp. 3700–3705), New York City, July.
Yildiz, Y., Annaswamy, A., Yanakiev, D., & Kolmanovsky, I. (2008a). Adaptive air fuel ratio control for internal combustion engines. In *Proceedings of the American control conference* (pp. 2058–2063), Seattle, Washington, June.
Yildiz, Y., Annaswamy, A., Yanakiev, D., & Kolmanovsky, I. (2008b). Automotive powertrain control problems involving time delay: An adaptive control approach. In *Proceedings of the ASME dynamic systems and control conference*, Ann Arbor, Michigan, October.
Yildiz, Y., Annaswamy, A., Yanakiev, D., & Kolmanovsky, I. (accepted for publication) Spark ignition engine idle speed control: An adaptive control approach. ⟨http://web.mit.edu/aaclab/publications/index.html⟩.
Zhang, F., Grigoriadis, K., Franchek, M., & Makki, I. (2007). Linear parameter varying lean burn air–fuel ratio control for a spark ignition engine. *Journal of Dynamic Systems, Measurement, and Control*, 129(4), 404–414.